

Individual Scatterers as Microscopic Origin of Equilibration between Spin-polarized Edge Channels in the Quantum Hall regime

Y. Acremann, T. Heinzel, and K. Ensslin

Solid State Physics Laboratory, ETH Zürich, 8093 Zürich, Switzerland

E. Gini and H. Melchior

Institute of Quantum Electronics, ETH Zürich, 8093 Zürich, Switzerland

M. Holland

Department of Electronics, University of Glasgow, Glasgow G12 8QQ, United Kingdom

(October 8, 2018)

The equilibration length between spin-polarized edge states in the Quantum Hall regime is measured as a function of a gate voltage applied to an electrode on top of the edge channels. Reproducible fluctuations in the coupling are observed and interpreted as a mesoscopic fingerprint of single spin-flip scatterers which are turned on and off. A model to analyze macroscopic edge state coupling in terms of individual scatterers is developed, and characteristic values for these scatterers in our samples are extracted. For all samples investigated, the distance between spin-flip scatterers lies between the Drude and the quantum scattering length.

The unique transport properties of two-dimensional electron gases in the integer Quantum Hall regime [1] can, to a large extent, be explained in a single particle picture by electronic transport via edge channels [2], which carry the current without dissipation over macroscopic distances. The Quantum Hall effect is not influenced by scattering between edge channels running at the same side of the sample. Such scattering, however, does occur and can be detected in various ways, for example by measuring the equilibration between edge channels [3]. In a macroscopic picture, the equilibration between two edge channels can be described by the coupling P , a macroscopic quantity defined by $P = (\Delta\mu - \Delta\mu')/\Delta\mu$, where $\Delta\mu$ and $\Delta\mu'$ are the differences in the electrochemical potential between the edge channels before and after the equilibration along a length L . The equilibration length ℓ_{eq} is then defined by the length over which $\Delta\mu$ is reduced to $1/e$ of its initial value, i.e. $\ell_{eq} = -L/\ln(1 - P)$ [3].

This picture does not contain information on the microscopic origin of edge state equilibration. However, it is generally accepted that equilibration between spin-polarized edge channels, separated in energy by $g\mu_B B$ (g is the effective electronic g-factor, μ_B the Bohr magneton, and B the magnetic field) takes place via spin-orbit coupling [3], in contrast to the equilibration between edge channels separated in energy by the Landau gap [4]. Impurities provide magnetic field gradients in the reference frame of the moving electrons, which can induce scattering between edge channels of opposite spin. Measurements of the equilibration length over macroscopic distances [5,6] are in agreement with the values obtained from the theory of this spin-orbit coupling mechanism [7–11]. Other possible mechanisms for inter-edge state coupling, for example magnetic impurities, are thought to play only a secondary role in clean Ga[Al]As heterostruc-

tures. In a recent work, Polyakov [12] argues that since these spin-flip transitions involve a momentum transfer to the impurity potential, their rate must be suppressed when the disorder is smooth. He concludes that the spin-flip scattering is not only very sensitive to the local potential, but also that transitions are induced by rather rare fluctuations which provide a strong scattering potential. It is precisely this picture that we can support by the measurements presented here. Basically, we study the edge channel equilibration on a length scale short enough that fluctuations due to individual scatterers do not average out. By comparing the coupling induced by individual scatterers with the macroscopic coupling, we determine a spin-flip scattering length ℓ_{sf} , i.e. the distance between scatterers leading to a coupling between the spin-resolved edge channels. We find that in all our samples, this length is smaller than the Drude scattering length, but significantly larger than the quantum scattering length.

The samples under study are standard Ga[Al]As heterostructures (see Table 1, upper part, for their properties). A Hall bar geometry is defined by wet chemical etching, and the electron gas is accessed via Ni-AuGe Ohmic contacts (inset in Fig.1). Each sample contains three gates, two of which cross the Hall bar (referred to as gate 1 and gate 2), and a third one (referred to as edge gate - eg) is located in between gates 1 and 2. The edge gate crosses one of the mesa edges and extends $2\ \mu\text{m}$ onto the mesa. In order to observe a possible effect of individual scatterers on the edge state coupling, the length L of the edge gate was chosen to be of the order of the equilibration length ℓ_{eq} between the spin-polarized edge states 1 and 2, which was determined in previous studies to be of the order of $24\ \mu\text{m}$. The samples were cooled down to the base temperature $T < 100\text{mK}$ of a dilution refrigerator. A magnetic field was applied

perpendicular to the electron gas to establish filling factor (i.e. the number of occupied Landau levels) 2 in the ungated regions, and the longitudinal resistance R_{xx} as a function of gate voltages is measured using a standard lock-in technique (a current of 10 nA at a frequency of 13 Hz). The electron densities and mobilities can be found in Table 1. Fig. 1 shows a measurement of ℓ_{eq} for sample A1163. First, V_1 is swept while $V_2 = V_{eg} = +55mV$. For $+100mV > V_1 > -100mV$, R_{xx} is essentially zero, indicating perfect transmission of both edge channels. Between $V_1 = -100mV$ and $V_1 = -160mV$, R_{xx} increases to $0.5h/e^2$. The spin-down channel is now completely reflected. At even lower voltages ($V_1 < -300mV$, the spin-up channel gets also reflected and R_{xx} approaches infinity [13]. We then sweep V_2 while keeping V_1 fixed at $V_1 = -215mV$, and $V_{eg} = +55mV$. Again, the spin-down channel is reflected around $V_2 = -160mV$. However, R_{xx} is only $0.78h/e^2$, which is a measure for the edge state equilibration. This setup for measuring ℓ_{eq} has been used before by Müller et al [10]. Using the expressions derived in Ref. [10], we find $\ell_{eq} = 18.7\mu m$, and a coupling of $P = 0.72$ for sample A1163.

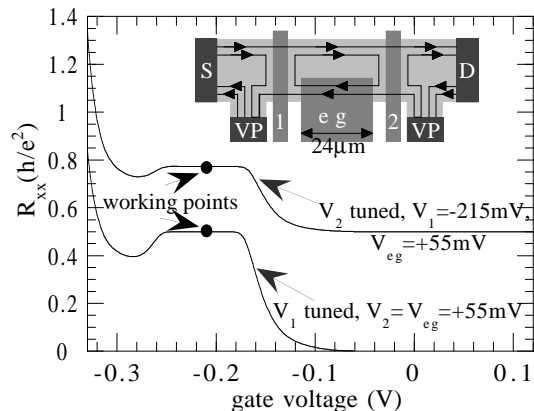


FIG. 1. R_{xx} of sample A1163 as a function of the voltages applied to gates 1 and 2, respectively, in a magnetic field of $B = 9.3T$, applied perpendicular to the electron gas. The inset shows a scheme of the Hall bar geometry used. Dark areas denote Ohmic contacts used as source (S), drain (D), and voltage probes (VP) to the electron gas (light grey). In addition, 3 gates are used, gate 1, gate 2 and the edge gate (eg). Two edge channels are present, of which the spin-down channel gets completely reflected at gates 1 and 2, when they are biased to the working point of $-215 mV$.

In the following, we focus on a voltage applied to the edge gate that influences the coupling between the edge channels. For these experiments, both gate 1 and 2 are biased at a constant voltage of $V_{1,2} = -215mV$, i.e. the spin-down channel is reflected at both gates. If we assume that the edge channel coupling below the edge gate, P_{eg} , can be different than the edge channel coupling P_u along the ungated edge, R_{xx} is determined by P_{eg} and P_u . Using the Landauer-Büttiker formalism [14], one finds:

$$R_{xx} = \frac{h}{2e^2} \frac{P_{eg} + P_u}{P_{eg} + P_u - P_{eg} \cdot P_u} \quad (1)$$

For $P_{eg} = P_u = P$, eq. 1 reduces to the standard expression, i.e. $R_{xx} = (h/e^2)/(2 - P)$ [10]. Fig. 2a shows R_{xx} as a function of the edge gate voltage V_{eg} with $V_{1,2} = -215mV$, clearly indicating that the edge state coupling depends upon V_{eg} (eq. 1). For $V_{eg} > -100mV$, the coupling is reduced when the gate voltage is lowered. Here, lowering V_{eg} reduces the electron density underneath the edge gate, resulting in an increasing separation between the edge channels and their continuous shift away from the mesa edge. Pronounced, reproducible fluctuations are visible in this regime (Fig. 2b), which we will discuss below in detail. At $V_{eg} = -100mV$, a sharp drop in the coupling occurs. Using $P_u = 0.72$ from above, P_{eg} drops to 0.56 in the minimum, which means that ℓ_{eq} increases to $30\mu m$ for the edge channels below the gate. At $V_{eg} = -100mV$, the spin-down channel is excluded from the gated area, as it happens below gates 1 and 2 (see Fig. 1) at a similar voltage, and the edge channel separation reaches its maximum. A further reduction of V_{eg} shifts only the spin-up channel towards the edge of the gated region while leaving the spin-down channel basically unaffected. As below gates 1 and 2, the electron gas is completely depleted underneath the edge gate around $V_{eg} = -300mV$, and both edge channels run again in close proximity outside the region covered by the edge gate. Consequently, the coupling jumps back up at $V_{eg} = -300mV$.

The resistance fluctuations occur in the regime between $-100mV \leq V_{eg} \leq +150mV$ and are perfectly reproducible in each sample (Fig. 2b) for different sweeps of V_{eg} , while their amplitude and characteristic period depend upon the heterostructure used. No indication for similar fluctuations could be found as a function of V_1 or V_2 . Typically, the fluctuation amplitude is of the order of 50Ω in our samples, and their period is of the order of 10 mV in V_{eg} . They vanish at a temperature of roughly 1K. We interpret these fluctuations as the effect of single impurities, each of which contributes an average inter-edge state coupling q . Since the edge gate voltage varies the energy and the position of the edge channels, single scatterers can be switched on and off. In this interpretation, the fluctuations can be viewed as a mesoscopic fingerprint of the spin-flip scatterers under the edge gate. Within our picture, we can obtain the average coupling induced by a single scatterer by analyzing the amplitude of the fluctuations, and their period gives information about the typical energy range over which one scatterer effects the edge state coupling.

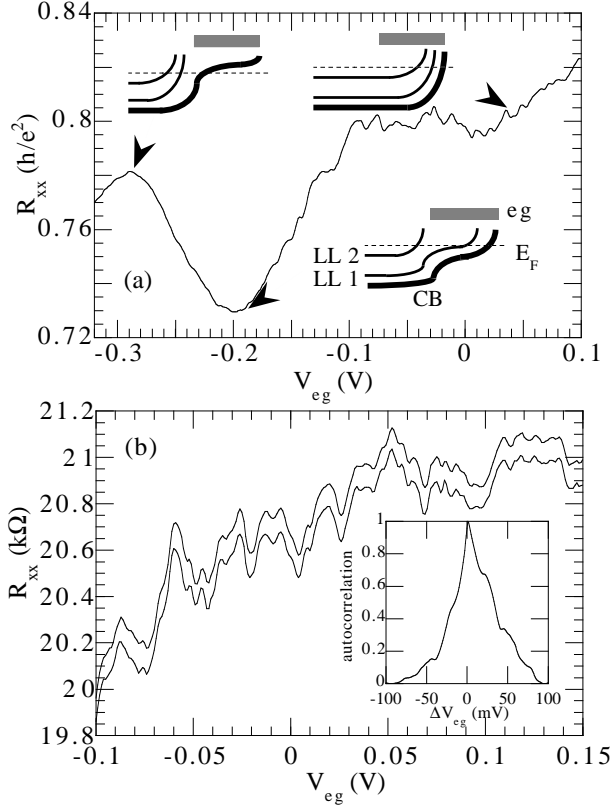


FIG. 2. a) R_{xx} as a function of the edge gate voltage, as measured on sample A1163, reflecting the variation of the inter-edge state coupling. The insets sketch the energy of Landau levels 1 and 2 in the corresponding regimes, indicating their gradual exclusion from the gated region as the edge gate voltage is reduced. E_F denotes the Fermi energy, and CB the bottom of the conduction band. b) Reproducible fluctuations in the regime between $-100\text{mV} \leq V_{eg} \leq +150\text{mV}$. The traces are offset by 100Ω for clarity. The inset shows the autocorrelation function as a function of the voltage shift of these fluctuations.

The average fluctuation in edge state coupling is calculated from the average fluctuation in R_{xx} using a simple model described below. A relation between the resistance fluctuations and q is derived (eq. 6). Once q is known, the number of scatterers N under the edge gate leading to equilibration can be calculated (eq. 4), and hence ℓ_{sf} , given by $\ell_{sf} = L/N$, is obtained. Here, L denotes the length of the edge gate. Tuning V_{eg} changes P_{eg} while leaving P_u unchanged. Assuming that P_{eg} is produced by N individual inter-edge state scatterers, each with an average coupling q , we can define q as $q = 1 - (\Delta\mu_i/\Delta\mu_{i-1})$, in analogy to the definition of P in Ref. [3]. Here, $\Delta\mu_i$ denotes the difference in the electrochemical potential between the two edge channels after they have felt i active scatterers. We will denote the coupling provided by N scatterers as $P_{eg,N}$. As a consequence of edge state coupling, the difference in the electrochemical potentials of

the edge channels at the entrance of the edge gate $\Delta\mu_0$ is reduced along the gated edge, finally reaching $\Delta\mu_N$. Hence, we can rewrite the definition of the edge state coupling as

$$P_{eg,N} = 1 - (\Delta\mu_N/\Delta\mu_0) \quad (2)$$

Using the above equation for defining q iteratively, $\Delta\mu_N$ can be written as

$$\Delta\mu_N = \Delta\mu_0 \cdot (1 - q)^N \quad (3)$$

We find N by inserting (3) in (2):

$$N = \frac{\ln(1 - P_{eg,N})}{\ln(1 - q)} \quad (4)$$

Furthermore, we can calculate how one additional scatterer changes $P_{eg,N}$. Inserting (3) in (2) for N and for $N + 1$ scatterers, we get

$$P_{eg,N+1} = P_{eg,N} + q - q \cdot P_{eg,N} \quad (5)$$

Using (5), we can calculate how R_{xx} is changed by adding one scatterer. For simplicity, we set $P_{eg,N} = P_u = P$, a reasonable estimate in the regime $-100\text{mV} < V_{eg} < 100\text{mV}$ (see Fig. 2a). In order to obtain q from the fluctuations in R_{xx} , we calculate $\Delta R_{xx} = \Delta R_{xx,N+1} - \Delta R_{xx,N}$ by inserting $P_{eg,N+1}$ and $P_{eg,N}$ from eqns. (5) and (2) in (1) and find $q = \Delta R_{xx} \cdot (P - 2)^2 P / ((P - 1)\Delta R_{xx} \cdot (2 - 3P + P^2) - P \cdot h/2e^2)$. Since the first term in the denominator is always small compared to the second one for our measurements, we can approximate

$$q \approx \frac{2e^2}{h} \cdot \Delta R_{xx} \cdot (2 - P)^2 \quad (6)$$

We have investigated 3 Ga[Al]As heterostructures named A1163, A577 and R2065. Samples A1163 and A577 have been grown by molecular beam epitaxy, MBE, with different layer sequences. In sample A1163, a rather high electron density is realized, while in sample A577, the sheet density is much lower (see Table 1). Both samples show Drude scattering lengths (as extracted from the electron density and the mobility at $B=0$) of the order of $3\mu\text{m}$ and quantum scattering lengths (obtained by fitting the Shubnikov-de Haas oscillations to the formula given by Ando et al. [15]) of the order of 100nm . The sample with the higher mobility (A577) also shows a higher equilibration length. In addition, sample R2065 has been grown by metal organic chemical vapor deposition (MOCVD). Both Drude and quantum scattering length are one order of magnitude smaller in sample R2065, and ℓ_{eq} is reduced as well. The two MBE grown samples show large q values of the order of 0.02 , while the low-mobility sample R2065, has only $q = 0.0064$, but there are much more spin-flip scatterers. Both N and q scale monotonically with the Drude as well as on the

quantum scattering length. The results for q and the number of scatterers N in each sample are summarized in Table 1. We find that ℓ_{sf} lies significantly below the Drude scattering length, but also significantly above the quantum scattering length in all our samples. We conclude that the electric field of a spin-flip scatterer is well below that one of a large-angle scatterer, but also well above that one of a small-angle scatterer. Our data also indicate that by increasing the number of spin-flip scatterers, the effective coupling per scatterer decreases and ℓ_{sf} approaches the quantum scattering length when N is increased. When the sample gets dirtier, more scatterers contribute to spin-flip scattering, but each one with a reduced strength. This could mean that the potential gradients of different scatterers tend to cancel each other when the scatterer density is increased. Hence, we see that in order to observe the fluctuations in the edge state coupling, it is essential to choose the gate length not too large compared to ℓ_{sf} , in order to avoid a complete canceling of the resistance fluctuations. Furthermore, we have studied the typical energy range over which spin-flip scatterers are active. In the inset in Fig. 2b, the autocorrelation function of the fluctuations vs. V_{eg} is shown. To translate the measured autocorrelation voltages in energies, we determine the lever arm α of the edge gate as $\alpha = \Delta E / \Delta V_{eg}$ from the pinch off voltage needed for complete depletion of the electron gas, i.e. $\alpha = E_F / (V_0 - V_{pinch-off})$. In other words, the energy is changed by the Fermi energy if the voltage is varied from $V_0 = +55mV$ down to the pinch-off voltage of $-320mV$. We find correlation energies E_C of the order of $100\mu eV$ for our samples A577 and R2065, and a somewhat higher value of $700\mu eV$ for sample A1163. We can estimate E_C / ℓ_{sf} as a lower limit for the typical electric field of an impurity leading to edge state equilibration, and find values of the order of $10^3 V/m$, which is roughly one order of magnitude below the characteristic electric field of a Drude scatterer, screened by the electron gas [16]. This number for the electric field is, however, no more than a crude estimate, since the effect of V_{eg} on the spatial position of the edge states is neglected.

In conclusion, we have investigated the microscopic origin of edge channel equilibration in two-dimensional electron gases. By tuning the edge channels in space and energy via a gate voltage, we observe reproducible fluctuations of the edge state equilibration, which we interpret as the turning on and off of individual spin-flip scatterers. We have provided the framework to analyze these fluctuations in order to extract characteristic numbers, such as the edge state coupling a single scatterer induces and the average distance between such scatterers. Our analysis supports recent theoretical work, i.e. that spin-flip scattering is caused by only a few, but rather strong, scattering potentials.

The authors would like to thank T. Ihn for valuable

discussions. Financial support from the Schweizerischer Nationalfonds is gratefully acknowledged.

TABLE I.

Characteristics of the samples under study. Upper part: data obtained from magnetotransport experiments. Lower part: numbers related to the inter-edge channel scattering.

sample	A1163	A577	R2065
electron density ($10^{15} m^{-2}$)	4.5	2.7	2.0
mobility (m^2/Vs)	60	82	6.1
Drude scattering length (μm)	3.0	3.2	0.2
quantum scattering length (nm)	82	92	25
equilibration length ℓ_{eq} (μm)	18.7	29.3	13.8
average fluctuation $\Delta R_{xx} (h/e^2)$	0.0061	0.0047	0.0024
correlation energy (meV)	0.7	0.1	0.2
coupling q per impurity	0.020	0.019	0.0064
number N of spin-flip scatterers	63	42	270
spin-flip scattering length ℓ_{sf} (nm)	381	571	89

-
- [1] K.v. Klitzing, G. Dorda, and M. Pepper, Phys. Rev. Lett. **45**, 494 (1980); for a review, see The Quantum Hall Effect, eds. R.E. Prange and S.M. Girvin (Springer, New York 1987)
 - [2] B.I. Halperin, Phys. Rev. B **25**, 2185 (1982); M. Bttiker, Phys. Rev. B **38**, 9375 (1988)
 - [3] For a review, see R. J. Haug, Semicond. Sci. Technol. **8**, 131 (1993)
 - [4] B.W. Alphenaar, P.L. McEuen, R.G. Wheeler, and R.N. Sacks, Phys. Rev. Lett. **64**, 677 (1990)
 - [5] R.J.F. van Haren, P.A.P. Blom, W. de Lange, and J. H. Wolter, Phys. Rev. B **47**, 15700 (1993)
 - [6] J. Herfort, Y. Tagagaki, K.J. Friedland, R. Hey, H. Kostial, and K. Ploog, Phys. Rev. B **55**, 1357 (1997)
 - [7] S. Komiyama, H. Hirai, M. Oshawa, Y. Matsuda, S. Sasa, and T. Fujii, Phys. Rev. B **45**, 11085 (1992)
 - [8] H. Hirai, S. Komoyama, S. Fukatsu, T. Osada, Y. Shiraki, and H. Toyoshima, Phys. Rev. B **52**, 11159 (1995)
 - [9] A.V. Khaetskii, Phys. Rev. B **45**, 13777 (1992)
 - [10] G. Mller, D. Weiss, A.V. Khaetskii, K. v. Klitzing, S. Koch, H. Nickel, W. Schlapp, and R. Lsch, Phys. Rev. B **45**, 3932 (1992)
 - [11] T. Martin and S. Feng, Phys. Rev. B **44**, 9084 (1991)
 - [12] D.G. Polyakov, Phys. Rev. B **53**, 15777 (1996)
 - [13] R.J. Haug, A.H. MacDonald, P. Streda, and K.v. Klitzing, Phys. Rev. Lett. **61**, 2797 (1988), and Ref.1.
 - [14] M. Bttiker, Phys. Rev. B **38**, 9375 (1988)
 - [15] T. Ando, A.B. Fowler and F. Stern, Rev. Mod. Phys. **54/2**, 437 (1982)
 - [16] A. Gold, Phys. Rev. B **38**, 10798 (1988), and references therein